

Effects of damping on the linear stability of a free-free beam subjected to follower and transversal forces

O. Kavianipour[†]

Department of Aerospace Engineering, K. N. T. University of Technology, Tehran, Iran

S.H. Sadati[‡]

Department of Mechanical Engineering, K. N. T. University of Technology, Tehran, Iran

(Received April 29, 2009, Accepted September 29, 2009)

Abstract. In this paper a free-free uniform beam with damping effects subjected to follower and transversal forces at its end is considered as a model for a space structure. The effect of damping on the stability of the system is first investigated and the effects of the follower and transversal forces on the vibration of the beam are shown next. Proportional damping model is used in this work, hence, the effects of both internal (material) and external (viscous fluid) damping on the system are noted. In order to derive the frequency of the system, the Ritz method has been used. The mode shapes of the system must therefore be extracted. The Newmark method is utilized in the study of the system vibration. The results show that an increase in the follower and transversal forces leads to an increase of the vibrational motion of the beam which is not desirable.

Keywords: beam instability; non-conservative force; follower force; proportional damping; vibration analysis.

1. Introduction

Many problems are modeled by beams subjected to axial or follower forces. The stability of the beams under the axial or follower force is of vital importance and is of interest to many researchers in aerospace industry, as it can be applied to many aerospace structures. The direction of the axial force is assumed to be immovable while the direction of the follower force is always perpendicular to the cross surface of the beam and changes with the beam deflections. Axial or follower forces have a significant influence on the structural natural frequencies. The critical axial force normally causes the static instability (divergence) and the critical follower force may cause static or dynamic instability (flutter). Divergence happens when the vibration frequency of the system becomes zero and flutter occurs when two natural frequencies of the systems converge together.

In this paper, an aerospace structure is modeled by a Bernoulli-Euler beam with proportional

[†] M.S. Student, Corresponding author, E-mail: o.kavianipour@gmail.com

[‡] Assistant Professor, E-mail: sadati@kntu.ac.ir

damping under the follower and transversal forces. This is an acceptable model for such structures with a propulsion force and a controller force. The latter is the force for the actuators to control and guide the aerospace structure to sustain a desired behavior. The main objective pursued in the paper is to determine the maximum follower force structurally bearable in such a way as to prevent instability of the structure. It will be shown that the proportional damping has a significant effect on this maximum follower force. It will also be shown that increasing the follower force or the transversal force results in an increase in the vibrational movement of the inertial measurement units (IMU). This in turn causes an inaccuracy in the guidance system and performance degradation in the actuators. The Ritz method is used in the calculations of the system frequencies and the Newmark method is employed for the study of the vibrational properties of the model.

Bokaian (1988) obtained an analytical characteristic equation for uniform beams under constant compressive axial load and considered some approximate relations for the buckling load and variation of normalized natural frequency with normalized axial force. Thana and Ameen (2007) addressed the dynamic stability problem of columns and frames subjected to the axially-applied periodic loads. The finite element method (FEM) was used in their work to analyze dynamic stability problems of columns. Hassanpour *et al.* (2007) analyzed the exact solution of free vibration of a beam with a concentrated mass within its intervals when the beam was subjected to axial loadings. They determined the exact mode shapes of vibration, which were necessary in the study and analysis of the time-domain response of sensors and determination of stability regions.

Joshi (1995) established a simple method to determine the mode shapes and the natural frequencies of a non-uniform beam subjected to rear end propulsion force. Another research to obtain the governing vibration equations and the stability of a beam under axial force was carried out by Nihous (1997). Pourtakdoust and Assadian (2004) modeled a free-free Bernoulli-Euler beam under an axial force. The three dimensional elastic equations of vibration are solved by the FEM. Only the divergence was found and shown in their work. And finally the elastic equations along with the equations of motion were simulated in a controller loop by the authors in their last work. It has been shown that the oscillations of the actuators were increased when the axial force was applied.

Lee (1995) formulated the equation of motion in matrix form of a cantilever Bernoulli-Euler beam subject to a tip-concentrated follower force at the free end based on the Lagrangian approach and the assumed mode method. Zuo and Schreyer (1996) studied the instability of a cantilevered beam and a simply supported plate, subjected to a combination of fixed and follower forces. Langthjem and Sugiyama (1999) studied a cantilever beam under a follower force with a tip mass to optimize the design of the beam. Another research on the instability of a non-uniform cantilever beam under a follower force was done by Au *et al.* (1999) using finite element method. Langthjem and Sugiyama (2000) offered a survey of simple, flexible structural elements subjected to non-conservative follower loads. Detinko (2002) analyzed simple model of a slender beam loaded by a transverse follower force and undergoing a lateral flutter. Wang and Quek (2002) illustrated the use of a pair of piezoelectric layers in increasing the flutter and buckling capacity of a column subjected to a follower force. Kurnik and Przybyłowicz (2003) analyzed active stabilisation of self-excited vibration of slender rotating columns subject to tangential follower forces. Such systems exhibit flutter-type instability as a result of energy transfer from rotation and to transverse motion of the shaft. Young and Juan (2003) presented a study of non-linear response of a fluttered, cantilevered beam subjected to a random follower force at the free end. Wang (2004) presented a comprehensive analysis of the stability of a cracked beam subjected to a follower compressive load. Ravi Kumar *et al.*

(2005) dealt with the study of vibration and dynamic instability characteristics of laminated composite doubly curved panels, subjected to non-uniform follower load, using finite element approach. Luongo and Di Egidio (2006) studied an internally constrained planar beam, equipped with a lumped visco-elastic device and loaded by a follower force. Paolone *et al.* (2006) analyzed the stability of a cantilever elastic beam with rectangular cross-section under the action of a follower tangential force and a bending conservative couple at the free end. Elfelsoufi and Azrar (2006) presented a mathematical model based on integral equations for numerical investigations of stability analyses of damped beams subjected to sub-tangential follower forces. Many researchers have also published their work on cantilever beam under a follower force with damping (Ryu and Sugiyama (2003), Detinko (2003), Di Egidio *et al.* (2007), Lee *et al.* (2007), Katsikadelis and Tsiatas (2007), and Tsiatas and Katsikadelis (2009)). Sugiyama and Langthjem (2007) studied cantilever beam under a follower force with proportional damping. Both internal (material) and external (viscous fluid) damping were considered. Tomski *et al.* (2007) presented the results of theoretical and numerical studies on the slender, geometrically nonlinear system supported at the loaded end by a spring of a linear characteristic and subjected to non-conservative (generalized Beck's) loading. The large-deflection problem of a non-uniform spring-hinged cantilever beam under a tip-concentrated follower force was considered by Shvartsman (2007). Shape optimization was used to optimize the critical load of an Euler-Bernoulli cantilever beam with constant volume subjected to a tangential compressive tip load and/or a tangential compressive load arbitrarily distributed along the beam by Katsikadelis and Tsiatas (2007). De Rosa *et al.* (2008) dealt with the dynamic behavior of a clamped beam subjected to a sub-tangential follower force at the free end. Djondjorov and Vassilev (2008) have studied the dynamic stability of a cantilevered Timoshenko beam lying on an elastic foundation of Winkler type and subjected to a tangential follower force. Attard *et al.* (2008) have investigated the dynamic stability behaviors of damped Beck's columns subjected to sub-tangential follower forces using fifth-order Hermitian beam elements. Marzani *et al.* (2008) have applied the generalized differential quadrature (GDQ) method to solve classical and non-classical non-conservative stability problems. The governing differential equation for a non-uniform column subjected to an arbitrary distribution of compressive sub-tangential follower forces has been obtained.

Beal (1965) investigated a uniform free-free beam under an end follower force. He introduced a direction control mechanism for the follower force to eliminate the tumbling instability of a free-free beam under a follower force. He also showed that, in the absence of a control system, the magnitude of the critical follower force is associated with coalescence of the two lowest bending frequencies. When the control system was included, it was found that the magnitude of the critical follower force only corresponded to a reduction of the lowest frequency of zero. Wu (1975) studied the stability of a free-free beam under a controlled follower force by using finite element discretization with an adjoint formulation. Park and Mote, jr. (1984) studied the maximum controlled follower force on a free-free beam carrying a concentrated mass. They predicted the location and the magnitude of the additional concentrated mass and the location and the gain of the follower force direction control sensor that permit the follower force to be maximized for stable transverse motion of the beam. Park (1987) investigated a uniform free-free Timoshenko beam under an end follower force with controlled direction. A finite element model of the beam transverse motion in the plane was formulated through the extended Hamilton's principle. The analysis showed that the effects of the rotary inertia and shear deformation parameters on the stable transverse motion of the beam are significant in certain ranges. Sato (1991) developed the governing

equation of motion of a Timoshenko beam under a follower force using Hamilton's principle. Mladenov and Sugiyama (1997) dealt with the stability of a flexible space structure subjected to an end follower force. The model consisted of two viscoelastic beams interconnected by two kinds of joints. One of the joints was composed of a rotational viscoelastic spring while another one was a shear viscoelastic spring. Bending flutter or post-flutter divergence showed to occur depending on the joint rigidity and internal damping. Kim and Choo (1998) analyzed the dynamic stability of a free-free Timoshenko beam with a concentrated mass subjected to a pulsating follower force. The effects of axial location and translation inertia of the concentrated mass were studied. They also examined the change of combination resonance types, the relationship between critical forces and widths of instability regions, and the effect of shear deformation.

2. Mathematical modeling

Fig. 1 shows the assumed model for an aerospace structure. The propulsion force is modeled by a follower force and the transversal force represents the controller force, as shown. In this figure, x_s and x_{F_0} indicate the points on the beam for the locations of the sensors, corresponding to the locations of the inertial measurement units (IMU) and the controller force in the aerospace structure, respectively. The beam is assumed to be axially rigid and is a Bernoulli-Euler beam. The gravity force is also ignored.

In this paper, the proportional damping model is used for modeling the damping of the system. To consider the effect of damping in the beam equation, the Kelvin-Voigt model is utilized. According to Meirovitch (1997), the bending moment is expressed in the form

$$M(x, t) = EI \left[\frac{\partial^2 y(x, t)}{\partial x^2} + C_\alpha \frac{\partial^3 y(x, t)}{\partial t \partial x^2} \right] \quad (1)$$

where $M(x, t)$, t , EI , C_α , are the bending moment, time, bending stiffness, and internal damping coefficient, respectively.

The governing equation for the uniform Bernoulli-Euler beam with proportional damping is derived as follows

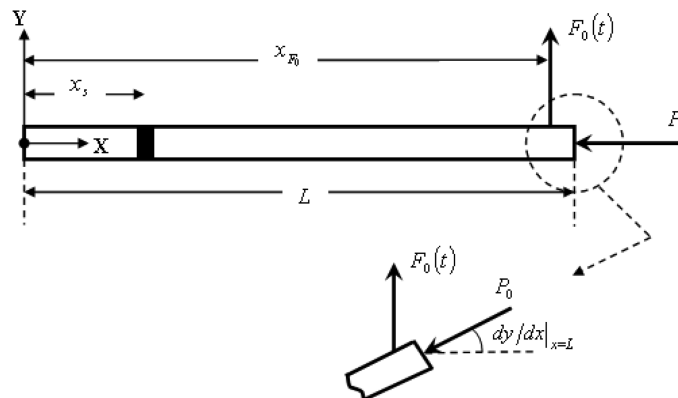


Fig. 1 A free-free beam subjected to follower and transversal forces

$$m \frac{\partial^2 y}{\partial t^2} + C_\beta \frac{\partial y}{\partial t} + C_\alpha EI \frac{\partial^5 y}{\partial t \partial x^4} + EI \frac{\partial^4 y}{\partial x^4} + \frac{\partial}{\partial x} \left(P(x) \frac{\partial y}{\partial x} \right) - F(x, t) = 0 \quad (2)$$

In this equation, m is the mass of the beam per unit length, C_β is the external damping coefficient, $P(x)$ is the axial force along the beam, and $F(x, t)$ is the lateral force per unit length.

To calculate the axial force along the beam, the equilibrium dynamics can be used as (Wu 1975)

$$P(x) = P_0 \frac{x}{L} \quad (3)$$

where P_0 is the follower force and L is the beam length.

In Fig. 1, one can consider that

$$F(x, t) = \frac{F_0(t) \delta(x - x_{F_0})}{L} \quad (4)$$

In this equation, x_{F_0} is the point at which the control force $F_0(t)$ is applied on the beam, and $\delta(x - x_{F_0})$ is the Dirac delta function.

To simplify the equations, non-dimensional parameters are introduced as the following

$$\begin{aligned} \bar{y} = \frac{y}{L}, \quad \bar{x} = \frac{x}{L}, \quad \bar{t} = t \left(\frac{EI}{mL^4} \right)^{0.5}, \quad \bar{P}_0 = \frac{P_0 L^2}{EI} \\ \bar{F}_0 = \frac{F_0(t) L^2}{EI}, \quad \bar{\beta} = C_\beta \left(\frac{L^4}{mEI} \right)^{0.5}, \quad \bar{\alpha} = C_\alpha \left(\frac{EI}{mL^4} \right)^{0.5} \end{aligned} \quad (5)$$

By substituting Eqs. (3), (4), and (5) in Eq. (2), Eq. (6) is obtained as the following

$$\frac{\partial^2 \bar{y}}{\partial \bar{t}^2} + \bar{\beta} \frac{\partial \bar{y}}{\partial \bar{t}} + \bar{\alpha} \frac{\partial^5 \bar{y}}{\partial \bar{t} \partial \bar{x}^4} + \frac{\partial^4 \bar{y}}{\partial \bar{x}^4} + \bar{P}_0 \frac{\partial}{\partial \bar{x}} \left(\bar{x} \frac{\partial \bar{y}}{\partial \bar{x}} \right) - \bar{F}_0 \delta(\bar{x} - \bar{x}_{F_0}) = 0 \quad (6)$$

As Eq. (6) shows, all the parameters in this equation are in non-dimensional form.

Considering the fact that the axial force distribution on the beam is not constant, the governing differential equation cannot be solved analytically and an approximation method must be used. It is noted that some approximation methods such as the Galerkin method (Hodges and Pierce 2002) need the governing equation of motion, which explains why Eq. (6) is introduced. In this study the Kantorovich method has been employed, which uses the Hamilton's principle (Hodges and Pierce 2002).

3. Ritz method

The general form of the Hamilton's Principle appears as

$$\delta \int_{\bar{t}_1}^{\bar{t}_2} (\bar{T} - \bar{V} + \bar{W}_c) d\bar{t} + \int_{\bar{t}_1}^{\bar{t}_2} d\bar{W}_{nc} d\bar{t} = 0 \quad (7)$$

where δ is the variation sign, \bar{t} is the non-dimensional time, \bar{T} is the non-dimensional kinetic energy, \bar{V} is the non-dimensional potential energy, \bar{W}_c is the non-dimensional work done by all conservative forces, and \bar{W}_{nc} is the non-dimensional work done by all non-conservative forces. For

the model shown in Fig. 1, Eq. (7) may be presented as

$$\left\{ \begin{aligned} \bar{T} &= \frac{1}{2} \int_0^1 \left(\frac{\partial \bar{y}}{\partial \bar{t}} \right)^2 d\bar{x} \\ \bar{V} &= \frac{1}{2} \int_0^1 \left(\frac{\partial^2 \bar{y}}{\partial \bar{x}^2} \right)^2 d\bar{x} \\ \bar{W}_c &= \frac{1}{2} \bar{P}_0 \int_0^1 \bar{x} \left(\frac{\partial \bar{y}}{\partial \bar{x}} \right)^2 d\bar{x} \\ \delta \bar{W}_{nc} &= \underbrace{- \int_0^1 \left[\bar{\beta} \frac{\partial \bar{y}}{\partial \bar{t}} \delta \bar{y} + \bar{\alpha} \frac{\partial^3 \bar{y}}{\partial \bar{t} \partial \bar{x}^2} \delta \left(\frac{\partial^2 \bar{y}}{\partial \bar{x}^2} \right) \right] d\bar{x}}_{\delta \bar{W}_{nc1}} - \underbrace{\bar{P}_0 \left(\frac{\partial \bar{y}}{\partial \bar{x}} \right) \Big|_{\bar{x}=1}}_{\delta \bar{W}_{nc2}} \delta \bar{y} \Big|_{\bar{x}=1} + \underbrace{\bar{F}_0 \delta \bar{y} \Big|_{\bar{x}=\bar{x}_{F_0}}}_{\delta \bar{W}_{nc3}} \end{aligned} \right. \quad (8)$$

In the Ritz method, the response is approximated with a series as the following

$$\bar{y}(\bar{x}, \bar{t}) = \sum_{i=1}^N \varphi_i(\bar{x}) q_i(\bar{t}) \quad (9)$$

where $\varphi_i(\bar{x})$ is assumed an admissible function and $q_i(\bar{t})$ is a generalized coordinate.

Substitution of Eq. (9) in Eq. (8), and then by substituting the result in Eq. (7), one arrives at

$$[M_{ij}][\ddot{q}_j] + [C_{ij}][\dot{q}_j] + [K_{ij}][q_j] = [Q_j] \quad (10)$$

where $\ddot{q}_j = d^2 q_j / d\bar{t}^2$ and $\dot{q}_j = dq_j / d\bar{t}$, $[M_{ij}]$ is the mass matrix, $[C_{ij}]$ is the damping matrix, $[K_{ij}]$ is the stiffness matrix, and $[Q_j]$ is the generalized force vector described as

$$\left\{ \begin{aligned} M_{ij} &= \int_0^1 \varphi_i \varphi_j d\bar{x} \\ C_{ij} &= \int_0^1 [\bar{\beta} \varphi_i \varphi_j + \bar{\alpha} \varphi_i'' \varphi_j''] d\bar{x} \\ K_{ij} &= \int_0^1 \varphi_i'' \varphi_j'' d\bar{x} - \bar{P}_0 \int_0^1 \bar{x} \varphi_i' \varphi_j' d\bar{x} + \bar{P}_0 \varphi_i'(1) \varphi_j(1) \\ Q_j &= \bar{F}_0 \varphi_j(\bar{x}_{F_0}) \end{aligned} \right. \quad (11)$$

where $\varphi_i'' = d^2 \varphi_i / d\bar{x}^2$ and $\varphi_i' = d\varphi_i / d\bar{x}$.

As a common rule, in the approximate solution methods, a partial differential equation may be put into a set of ordinary differential equations.

One remarkable point here is that the damping matrix of the system (using proportional damping model) does not appear as $[C_{ij}] = \bar{\beta}[M_{ij}] + \bar{\alpha}[K_{ij}]$, and a part of the stiffness matrix of the system that consists of the follower force (geometrical stiffness) does not enter in the damping matrix of the system. So

$$[C_{ij}] = \bar{\beta}[M_{ij}] + \bar{\alpha}([K_{ij}] - [K_{ij}^G]) \quad (12)$$

For which the geometrical stiffness matrix can be expressed as

$$K_{ij}^G = -\bar{P}_0 \int_0^1 \bar{x} \varphi_i' \varphi_j' d\bar{x} + \bar{P}_0 \varphi_i'(1) \varphi_j(1) \quad (13)$$

3.1 Admissible functions

In general, the admissible functions $\varphi(\bar{x})$ must satisfy the following four conditions:

- 1) At least must satisfy all geometric boundary conditions.
- 2) Must be continuous and differentiable to highest spatial derivative.
- 3) Should be a complete function.
- 4) Must be linearly independent.

The mode shapes of a free-free beam with proportional damping satisfy the above conditions and have been used in this study. As the first two rigid body modes are not involved in the instability, they are not considered as the admissible functions (Beal 1965).

To obtain the bending mode shapes of a uniform free-free Bernoulli-Euler beam with damping effects, the free vibration analysis was used ($\bar{P}_0 = 0$ and $\bar{F}_0 = 0$ in Eq. (6)). Hence, the equation

$$\frac{\partial^2 \bar{y}}{\partial \bar{t}^2} + \bar{\beta} \frac{\partial \bar{y}}{\partial \bar{t}} + \bar{\alpha} \frac{\partial^5 \bar{y}}{\partial \bar{t} \partial \bar{x}^4} + \frac{\partial^4 \bar{y}}{\partial \bar{x}^4} = 0 \quad (14)$$

is solved with the boundary conditions stated as

$$\begin{cases} \frac{\partial^2 \bar{y}}{\partial \bar{x}^2} + \bar{\alpha} \frac{\partial^3 \bar{y}}{\partial \bar{t} \partial \bar{x}^2} = 0 \\ \frac{\partial^3 \bar{y}}{\partial \bar{x}^3} + \bar{\alpha} \frac{\partial^4 \bar{y}}{\partial \bar{t} \partial \bar{x}^3} = 0 \end{cases} \quad \text{at } \bar{x} = 0, \bar{x} = 1 \quad (15)$$

The solution of Eq. (14) is considered as

$$\bar{y}(\bar{x}, \bar{t}) = \chi(\bar{x}) \tau(\bar{t}) = \chi(\bar{x}) e^{\lambda_0 \bar{t}} \quad (16)$$

By substituting Eq. (16) in Eq. (14), the equation below is obtained as

$$\lambda_0^2 \chi + \lambda_0 (\bar{\beta} \chi + \bar{\alpha} \chi''''') + \chi'''' = 0 \quad (17)$$

The boundary conditions of Eq. (15) become

$$\begin{cases} (1 + \lambda_0 \bar{\alpha}) \chi'' = 0 \\ (1 + \lambda_0 \bar{\alpha}) \chi'''' = 0 \end{cases} \quad \text{at } \bar{x} = 0, \bar{x} = 1 \quad (18)$$

where $\chi'''' = d^4 \chi / d\bar{x}^4$, $\chi'''' = d^3 \chi / d\bar{x}^3$, and $\chi'' = d^2 \chi / d\bar{x}^2$.

Simplifying Eqs. (17) and (18) leads to Eq. (19) and boundary condition (20) as follows

$$\chi'''' - \gamma^4 \chi = 0, \quad \gamma^4 = -\left(\frac{\lambda_0^2 + \lambda_0 \bar{\beta}}{1 + \lambda_0 \bar{\alpha}} \right) \quad (19)$$

$$\begin{cases} \chi'' = 0 \\ \chi''' = 0 \end{cases} \quad \text{at } \bar{x} = 0, \bar{x} = 1 \quad (20)$$

The characteristic equation and the solution of Eq. (19) subject to the boundary condition (20) are given in Eqs. (21) and (22), respectively.

$$\cos \gamma \cosh \gamma = 1 \quad (21)$$

$$\chi(\bar{x}) = \sin \gamma \bar{x} + \sinh \gamma \bar{x} + \left(\frac{\cos \gamma - \cosh \gamma}{\sin \gamma + \sinh \gamma} \right) (\cos \gamma \bar{x} + \cosh \gamma \bar{x}) \quad (22)$$

As shown in the above equations, the characteristic equation and bending mode shapes of a free-free uniform Bernoulli-Euler beam with proportional damping are not different from those obtained for the same beam without damping effects, but the frequencies of the two systems are different from each other.

$$\lambda_{0_1}, \lambda_{0_2} = \frac{-(\bar{\beta} + \bar{\alpha} \gamma^4)}{2} \pm \frac{\sqrt{(\bar{\beta} + \bar{\alpha} \gamma^4)^2 - 4\gamma^4}}{2} \quad (23)$$

The second term in the right-hand side of Eq. (23) illustrates the bending frequencies of a uniform free-free Bernoulli-Euler beam with proportional damping.

3.2 Solution

The most important objective of the present study is to determine the magnitude and type of the least follower force (the divergence or flutter) leading to instability \bar{P}_{0cr} . As seen in Eq. (11), the follower force affects the system stiffness matrix and changes the system frequencies. Therefore, to pursue the stated goal, one must first determine the system frequencies. To obtain the changes in the system frequencies in terms of the follower force, set the right hand side of Eq. (10) to zero ($\bar{F}_0 = 0$) and assume a homogeneous response as follows

$$[q_j] = [\hat{q}_j] e^{\lambda \tau}, \quad \lambda = \lambda_R + i \lambda_I, \quad i = \sqrt{-1} \quad (24)$$

where $[\hat{q}_j]$ is a vector with constant elements.

By substituting Eq. (24) in the homogeneous Eq. (10) and after some simplifications, the following matrix A is obtained. Clearly, the system frequencies are the eigenvalues of this matrix. Matrix A is

$$A = \begin{bmatrix} 0 & I \\ -[M_{ij}]^{-1} [K_{ij}] & -[M_{ij}]^{-1} [C_{ij}] \end{bmatrix} \quad (25)$$

where I is introduced as the identity matrix.

As for the results shown in the figures that follow, the parameter λ was divided by $\lambda_{0_{i1}}$ as

$$\bar{\lambda} = \left(\frac{\lambda}{\lambda_{0_{i1}}} \right) = \left(\frac{\lambda_R + i \lambda_I}{\lambda_{0_{i1}}} \right) = \bar{\lambda}_R + i \bar{\lambda}_I \quad (26)$$

where $\lambda_{0_{i1}}$ is the first frequency of uniform Bernoulli-Euler beam for the case that $\bar{P}_0 = 0$ (The second term in the right-hand side of Eq. (23) for γ_1).

To obtain the deflection of a point on the beam as shown in Fig. 1 (the distance \bar{x}_s from the tip of the beam ($\bar{x}_s = x_s/L$)), one must calculate the value of $q_i(\bar{t})$ used in Eq. (9). These parameters are calculated by solving Eq. (10) for which the Newmark method (Craig, Jr and Kurdila (2006)) is utilized in this paper. To solve the equations and obtain the results, the function $\chi(\bar{x})$ is used instead of the $\varphi(\bar{x})$. It is to be noted that in all the studies in this paper, as many as eight terms of the mode shapes are considered ($N=8$).

4. Numerical results and discussion

The results are discussed for several cases as follows.

4.1 $\bar{\alpha} = 0$ and $\bar{\beta} = 0$

To assure the validity of the computer code first, the case of $\bar{\alpha} = 0$ and $\bar{\beta} = 0$ is considered. In the first part, it is assumed that $\bar{F}_0 = 0$. The eigenvalues of the matrix A in Eq. (25) were calculated and illustrated in Figs. 2 and 3. As seen in Fig. 2, the value of the critical follower force is obtained as 109.8, which is very closely comparable with the value cited by Beal (1965), namely 109.9. By increasing the value of \bar{P}_0 , the values of $\bar{\lambda}_{I1}$ and $\bar{\lambda}_{I2}$ are changed and they will coincide each other at $\bar{P}_0 = 109.8$. It is precisely at this value of \bar{P}_0 at which $\bar{\lambda}_{R1}$ and $\bar{\lambda}_{R2}$ which are equal to each other take positive sign, hence ensuing instability at $\bar{P}_{0cr} = 109.8$. Since this value of \bar{P}_{0cr} makes the amplitude of vibration increase with time, the resulting instability is called dynamic instability or flutter. In Fig. 3, the variation of the first two eigenvalues of matrix A due to the variation of \bar{P}_0 is illustrated in a complex plane. It is shown in this figure that if the value of \bar{P}_0 increases, the eigenvalues of matrix A move to the right hand side of the complex plane, leading to instability. Note that in Fig. 3, only one significant figure after the decimal point was considered for the

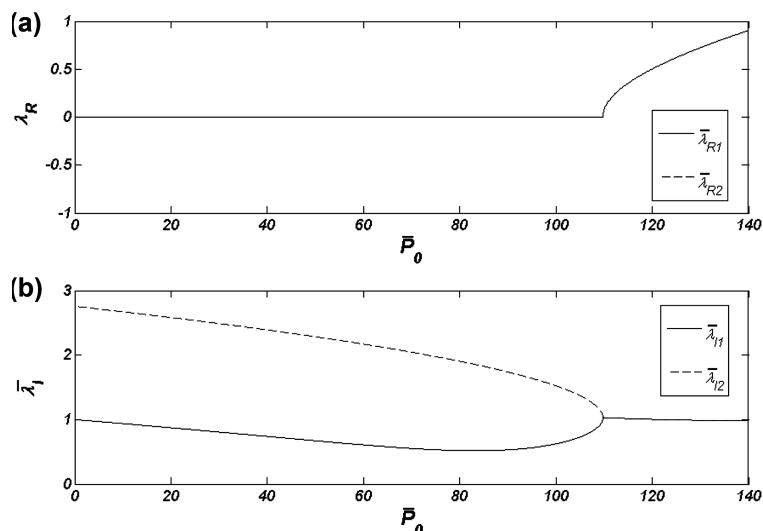


Fig. 2 Variation of the first two eigenvalues of matrix A due to the changes in \bar{P}_0 : (a) Real part of the eigenvalue, (b) Imaginary part of the eigenvalue

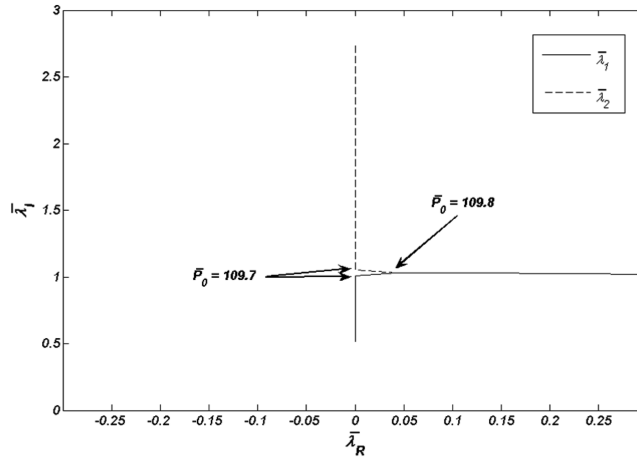


Fig. 3 Variation of the first two eigenvalues of matrix A due to the changes in \bar{P}_0 in the complex plane

accuracy of the \bar{P}_0 variation. If two significant figures after the decimal point had been considered instead, then the value would have been $\bar{P}_{0cr} = 109.73$.

4.2 $\bar{\alpha} \neq 0$ and $\bar{\beta} = 0$

In this section, the effect of $\bar{\alpha}$ alone on the critical follower force \bar{P}_{0cr} is investigated. In other words, the eigenvalues of matrix A (Eq. (25)) assuming $\bar{\beta} = 0$ and $F_0 = 0$ are calculated. As indeed shown in Fig. 4, with the smallest value considered for $\bar{\alpha}$ as $\bar{\alpha} = 10^{-6}$, the critical follower force leading to flutter is suddenly decreased from 109.73 to 88.2. For the $\bar{\alpha}$ values in the range $10^{-6} \leq \bar{\alpha} \leq 10^{-3}$, the value of the critical follower force remains constant. Conversely, in the range $10^{-3} < \bar{\alpha} \leq 10^{-1}$, the value of the critical follower force increased. The nature of these variations in a free-free beam is similar to that in a cantilever beam (Sugiyama and Langthjem 2007).

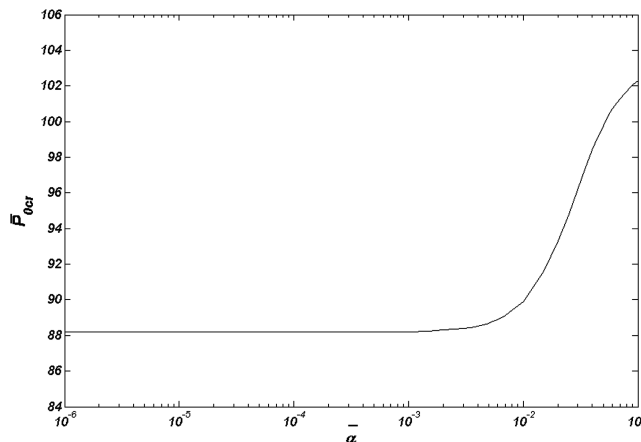


Fig. 4 Effect of $\bar{\alpha}$ on the value of \bar{P}_{0cr} (assuming $\bar{\beta} = 0$)

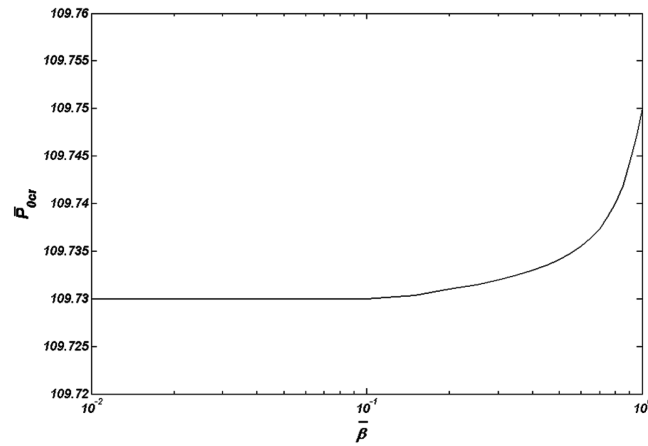


Fig. 5 Effect of $\bar{\beta}$ on the value of \bar{P}_{0cr} (assuming $\bar{\alpha} = 0$)

4.3 $\bar{\alpha} = 0$ and $\bar{\beta} \neq 0$

Here now, the effect of $\bar{\beta}$ alone on the critical follower force \bar{P}_{0cr} leading to flutter is investigated. The eigenvalues of matrix A are calculated considering $\bar{\alpha} = 0$ and $\bar{F}_0 = 0$. As seen in Fig. 5, small values of $\bar{\beta}$ within the range $10^{-2} \leq \bar{\beta} \leq 10^{-1}$, do not cause any change in the critical follower force and the value of this parameter remains unchanged at 109.73, the value obtained for the case of without damping effects. For the $\bar{\beta}$ values in the range $10^{-1} < \bar{\beta} \leq 10^0$, the value of the critical follower force increased. Although these variations are negligible in contrast with the previous case ($\bar{\beta} = 0, \bar{\alpha} \neq 0$), in this situation ($\bar{\beta} \neq 0, \bar{\alpha} = 0$), the value of the critical follower force is greater than the previous value calculated without damping effects ($\bar{\beta} = 0, \bar{\alpha} = 0$). The nature of these variations in a free-free beam is similar to that for a cantilever beam (Sugiyama and Langthjem 2007).

4.4 $\bar{\alpha} \neq 0$ and $\bar{\beta} \neq 0$

In this section, the simultaneous effects of $\bar{\alpha}$ and $\bar{\beta}$ together on the critical follower force \bar{P}_{0cr} leading to flutter are investigated. In fact, by considering $\bar{\beta} \neq 0$ and $\bar{\alpha} \neq 0$, and assuming $\bar{F}_0 = 0$, the eigenvalues of matrix A are calculated. As Fig. 6 shows, these two parameters affect the \bar{P}_{0cr} in different forms. In general, one can assert that there exists a specific value of $\bar{\alpha}$ at which increasing the $\bar{\beta}$ leads to a rise in the critical follower force, and that at a specific value of $\bar{\beta}$, an increase in the $\bar{\alpha}$ will at first lead to a decrease of the value of the critical follower force, and brings about a rise in this parameter later.

In Fig. 7, the variations of eigenvalues of matrix A (two first eigenvalue of matrix A) are illustrated for $\bar{\beta} = 0.1$ and $\bar{\alpha} = 0.001$ in the complex plane due to the variation of \bar{P}_0 (in this case $\bar{F}_0 = 0$). It is noted that a change in the value of \bar{P}_0 will move the eigenvalues from the left hand side of the complex plane to its right hand side. At $\bar{P}_0 = 90.9$, the real part of the eigenvalue becomes positive and so the critical follower force for this case equals to 90.9.

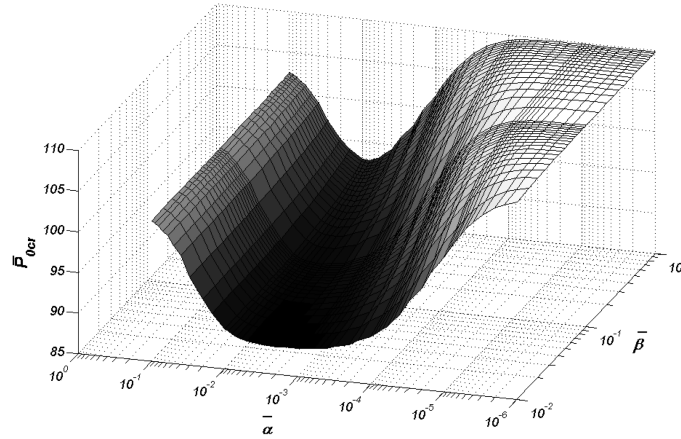


Fig. 6 Effect of $\bar{\alpha}$ and $\bar{\beta}$ on the value of \bar{P}_{0cr} (a study of the eigenvalues of matrix A assuming $\bar{\alpha} \neq 0$ and $\bar{\beta} \neq 0$)

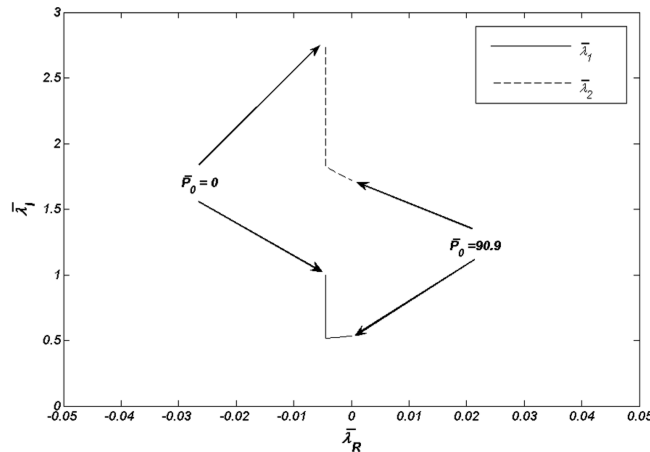


Fig. 7 Variation of the eigenvalue of matrix A (first two eigenvalues) due to the variation of \bar{P}_0 in the complex plane for $\bar{\beta} = 0.1$ and $\bar{\alpha} = 0.001$)

4.5 Vibration analysis

An important objective pursued here is to obtain the vibrational properties of a certain point of the structure \bar{x}_s due to the follower and transversal forces. To determine the vibrational motion $\bar{y}(\bar{x}_s, \bar{t})$, Eq. (9) shows that the value of $q_i(\bar{t})$ is required, which is in turn calculated from Eq. (10). The Newmark method is used to solve this equation. The assumptions are that $\bar{F}_0 = 0$, $\bar{\alpha} = 0.001$ and $\bar{\beta} = 0.1$. It is to be noted that for these parameter values, the critical follower force is $\bar{P}_{0cr} = 90.9$. Fig. 8 shows the vibrational properties with the $\bar{x}_s = 0.1$ as a function of time for a given initial condition. This is the case whereby $\bar{P}_0 = 9$. As shown in Fig. 8, the vibrational amplitude decreases with time. Fig. 8(d) depicts the trajectory for the \bar{x}_s , from which one can demonstrate stability of the system for this follower force using the Lyapunov's methods. Similar results were also obtained for the case of $\bar{P}_0 = 112$ presented in Fig. 9, which shows instability of the system.

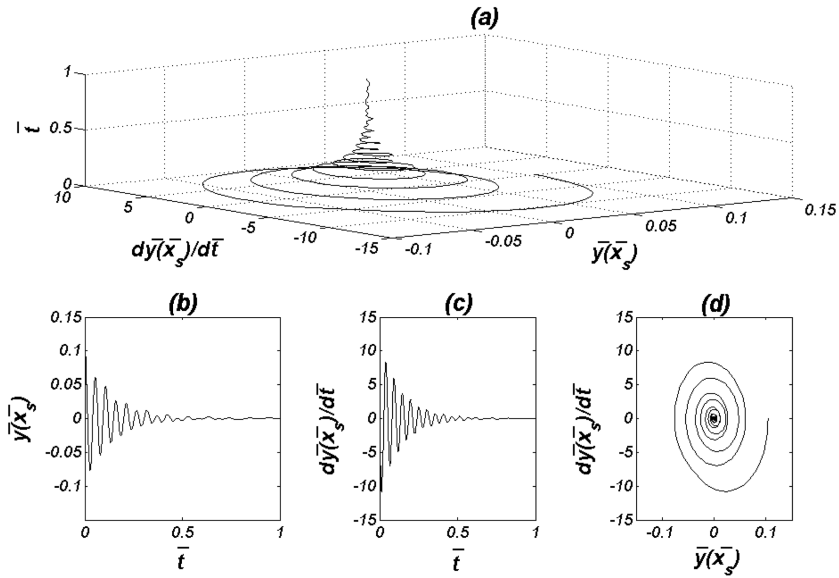


Fig. 8 Vibrational properties for the case of $\bar{P}_0 = 9$, $\bar{\alpha} = 0.001$, $\bar{\beta} = 0.1$ and $\bar{F}_0 = 0$ at point $\bar{x}_s = 0.1$

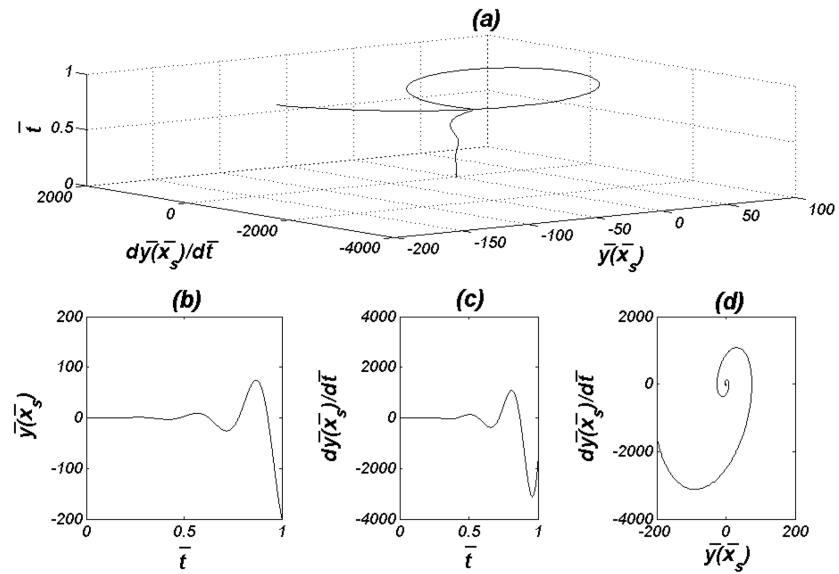


Fig. 9 Vibrational properties for the case of $\bar{P}_0 = 112$, $\bar{\alpha} = 0.001$, $\bar{\beta} = 0.1$ and $\bar{F}_0 = 0$ at point $\bar{x}_s = 0.1$

Fig. 10 shows the effect of the magnitude of the follower and transversal forces on the motion of the point $\bar{x}_s = 0.1$ assuming $\bar{\alpha} = 0.001$, $\bar{\beta} = 0.1$, $\bar{x}_{F_0} = 1$, $\bar{P}_0 = 5$, and $\bar{P}_0 = 50$ for the two different cases of $\bar{F}_0 = 0.001\sin(3\bar{t})$ and $\bar{F}_0 = 0.002\sin(3\bar{t})$. The magnitude of the transversal force is selected to be considerably smaller than that of the follower force. Moreover, the frequency is also taken to be smaller than that of the model. It is observed that increasing the follower or transversal force results in an increase in the motion of the \bar{x}_s of the beam. The \bar{x}_s can be considered to be the location of the IMU on the aerospace structure. This increase in vibrational

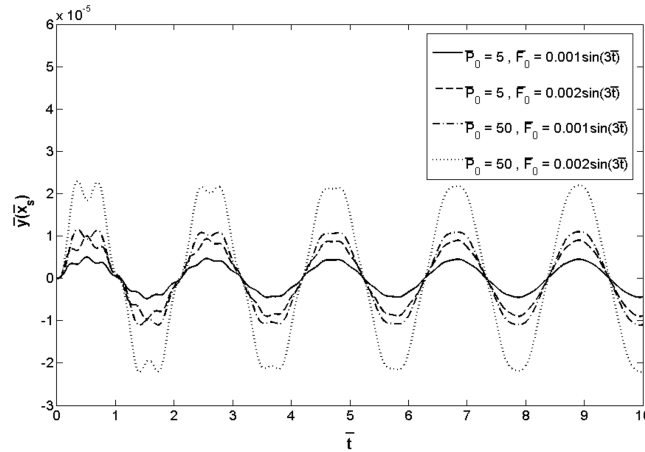


Fig. 10 Increase in the displacement of point $\bar{x}_s = 0.1$ due to the increase in the follower and transversal forces for the case of $\bar{\beta} = 0.1$, $\bar{\alpha} = 0.001$, $\bar{x}_{F_0} = 1$

motion is a destructive phenomenon for the control system of the aerospace structure and hence it must be remedied by proper approaches.

The results of Fig. 10 indicate that the oscillatory effects in the displacement at the \bar{x}_s position for the two values of \bar{P}_0 and \bar{F}_0 tend to eliminate in time due to the presence of damping effects. Moreover, the amplitude of displacement of the \bar{x}_s position tends to a fixed value. For a given set of values for \bar{P}_0 and \bar{F}_0 in time, point \bar{x}_s is displaced proportional to the amplitude and frequency of the excited force.

5. Conclusions

In this paper, a free-free uniform Bernoulli-Euler beam with proportional damping has been considered subjected to a follower force at the end and a transversal force at a specific point of the beam. The follower force is a model for the propulsion force and the transversal force represents the controller force. At first for the model without damping, the critical follower force leading to flutter was obtained as $\bar{P}_{0,cr} = 109.73$. It was also demonstrated that dynamic instability occurs since the eigenvalues of matrix A move to the right hand side of the complex plane. The dynamic instability due to an increase in the magnitude of \bar{P}_0 and in the presence of proportional damping occurred in the simulation results. In the case of $\bar{\alpha} \neq 0$ and $\bar{\beta} = 0$ for the smallest value of $\bar{\alpha}$, namely $\bar{\alpha} = 10^{-6}$, the critical follower force suddenly decreased from 109.73 to 88.2. In the range $10^{-6} \leq \bar{\alpha} \leq 10^{-3}$, the value of critical follower force remained constant, while in the range $10^{-3} < \bar{\alpha} \leq 10^{-1}$, the value of critical follower force increased. In this case, all the obtained critical follower forces cause flutter to occur. In the case of $\bar{\beta} \neq 0$ and $\bar{\alpha} = 0$, the small values of $\bar{\beta}$ in the range $10^{-2} \leq \bar{\beta} \leq 10^{-1}$ do not cause any change in the magnitude of the critical follower force, which remained in this order as for the no damping case, i.e., $\bar{P}_{0,cr} = 109.73$. In the range $10^{-1} < \bar{\beta} \leq 10^0$, the value of critical follower force increased (in fact, this type of damping alone has a stabilizing effect). In this case again, all the obtained critical follower forces caused flutter to occur. The dependence of the critical follower force on the internal damping factor becomes more complicated when external damping is also included ($\bar{\alpha} \neq 0$ and $\bar{\beta} \neq 0$). The different values of these two

parameters affect the \bar{P}_{0cr} in different manners. Generally, one can conclude that at a given value of $\bar{\alpha}$, increasing the value of $\bar{\beta}$ leads to a rise in the critical follower force, and that at a given value of $\bar{\beta}$, increasing the value of $\bar{\alpha}$ leads to a decrease in the value of the critical follower force at first, and then causes a rise in this parameter later. In this case again, all the obtained critical follower forces cause flutter to occur.

In general, increasing the follower or transversal force can lead to an increase in the vibration of the point \bar{x}_s (position of the measurement system on the aerospace structures) which is not desirable for a control system and hence it must be remedied by proper approaches. In the case in which the beam has a proportional damping, the oscillatory effects of the displacement at the \bar{x}_s position on the beam are damped out in time. But in the model without such damping, these oscillatory effects persist with time.

References

- Attard, M.M., Lee, J.S. and Kim, M.Y. (2008), "Dynamic stability of shear-flexible beck's columns based on Engesser's and Haringx's buckling theories", *Comput. Struct.*, **86**(21-22), 2042-2055.
- Au, F.T.K., Zheng, D.Y. and Cheung, Y.K. (1999), "Vibration and stability of non-uniform beams with abrupt changes of cross-section by using C1 modified beam vibration functions", *Appl. Math. Model.*, **29**, 19-34.
- Beal, T.R. (1965), "Dynamic stability of a flexible missile under constant and pulsating thrusts", *AIAA J.*, **3**(3), 486-494.
- Bokaian, A. (1988), "Natural frequencies of beam under compressive axial loads", *J. Sound Vib.*, **126**(1), 49-65.
- Craig, Jr., R.R. and Kurdila, A.J. (2006), *Fundamentals of Structural Dynamics*, John Wiley & Sons, Inc., New Jersey.
- De Rosa, M.A., Auciello, N.M. and Lippiello, M. (2008), "Dynamic stability analysis and DQM for beams with variable cross-section", *Mech. Res. Commun.*, **35**, 187-192.
- Detinko, F.M. (2002), "Some phenomena for lateral flutter of beams under follower load", *Int. J. Solids Struct.*, **39**, 341-350.
- Detinko, F.M. (2003), "Lumped damping and stability of Beck column with a tip mass", *Int. J. Solids Struct.*, **40**, 4479-4486.
- Di Egidio, A., Luongo, A. and Paolone, A. (2007) "Linear and non-linear interactions between static and dynamic bifurcations of damped planar beams", *Int. J. Non-linear Mech.*, **42**, 88-98.
- Djondjorov, P.A. and Vassilev, V.M. (2008), "On the dynamic stability of a cantilever under tangential follower force according to Timoshenko beam theory", *J. Sound Vib.*, **311**, 1431-1437.
- Elfeloufi, Z. and Azrar, L. (2006), "Integral equation formulation and analysis of the dynamic stability of damped beams subjected to subtangential follower forces", *J. Sound Vib.*, **296**, 690-713.
- Hassanpour, P.A., Cleghorn, W.L., Mills, J.K. and Esmailzadeh, E. (2007), "Exact solution of the oscillatory behavior under axial force of a beam with a concentrated mass within its interval", *J. Vib. Control*, **13**(12), 1723-1739.
- Hodges, D.H. and Pierce, G.A. (2002), *Introduction to Structural Dynamics and Aeroelasticity*, The Press Syndicate of the University of Cambridge, Cambridge.
- Joshi, A. (1995), "Free vibration characteristics of variable mass rocket having large axial thrust/acceleration", *J. Sound Vib.*, **187**(4), 727-736.
- Katsikadelis, J.T. and Tsiatas, G.C. (2007), "Optimum design of structures subjected to follower forces", *Int. J. Mech. Sci.*, **49**, 1204-1212.
- Katsikadelis, J.T. and Tsiatas, G.C. (2007), "Nonlinear dynamic stability of damped Beck's column with variable cross-section", *Int. J. Non-linear Mech.*, **42**(1), 164-171.
- Kim, J.H. and Choo, Y.S. (1998), "Dynamic stability of a free-free Timoshenko beam subjected to a pulsating follower force", *J. Sound Vib.*, **216**(4), 623-636.
- Kurnik, W. and Przybył owicz, P.M. (2003), "Active stabilisation of a piezoelectric fiber composite shaft subject to follower load", *Int. J. Solids Struct.*, **40**, 5063-5079.

- Langthjem, M.A. and Sugiyama, Y. (1999), "Optimum shape design against flutter of a cantilevered column with an end-mass of finite size subjected to a non-conservative load", *J. Sound Vib.*, **226**(1), 1-23.
- Langthjem, M.A. and Sugiyama, Y. (2000), "Dynamic stability of columns subjected to follower loads: A survey", *J. Sound Vib.*, **238**, 809-851.
- Lee, H.P. (1995), "Divergence and flutter of a cantilever rod with an intermediate spring support", *Int. J. Solids Struct.*, **32**(10), 1371-1382.
- Lee, J.S., Kim, N.I. and Kim, M.Y. (2007), "Sub-tangentially loaded and damped Beck's columns on two-parameter elastic foundation", *J. Sound Vib.*, **306**, 766-789.
- Luongo, A. and Di Egidio, A. (2006), "Divergence, Hopf and double-zero bifurcations of a nonlinear planar beam", *Comput. Struct.*, **84**, 1596-1605.
- Marzani, A., Tornabene, F. and Viola, E. (2008), "Nonconservative stability problems via generalized differential quadrature method", *J. Sound Vib.*, **315**, 176-196.
- Meirovitch, L. (1997), *Principles and Techniques of Vibrations*, Prentice-Hall International, Inc., New Jersey.
- Mladenov, K.A. and Sugiyama, Y. (1997), "Stability of a jointed free-free beam under end rocket thrust", *J. Sound Vib.*, **199**(1), 1-15.
- Nihous, G.C. (1997), "On the continuity of boundary value problem for vibrating free-free straight beams under axial loads", *J. Sound Vib.*, **200**(1), 110-119.
- Paolone, A., Vastab, M. and Luongoc, A. (2006), "Flexural-torsional bifurcations of a cantilever beam under potential and circulatory forces I. Non-linear model and stability analysis", *Int. J. Non-Linear Mech.*, **41**, 586-594.
- Park, Y.P. and Mote, Jr., C.D. (1984), "The maximum controlled follower force on a free-free beam carrying a concentrated mass", *J. Sound Vib.*, **98**(2), 247-256.
- Park, Y.P. (1987), "Dynamic stability of a free Timoshenko beam under a controlled follower force", *J. Sound Vib.*, **113**(3), 407-415.
- Pourtakdoust, S.H. and Assadian, N. (2004), "Investigation of thrust effect on the vibrational characteristics of flexible guided missiles", *J. Sound Vib.*, **272**, 287-299.
- Ravi Kumar, L., Datta, P.K. and Prabhakara, D.L. (2005), "Dynamic instability characteristics of laminated composite doubly curved panels subjected to partially distributed follower edge loading", *Int. J. Solids Struct.*, **42**, 2243-2264.
- Ryu, S.U. and Sugiyama, Y. (2003), "Computational dynamics approach to the effect of damping on stability of a cantilevered column subjected to a follower force", *Comput. Struct.*, **81**, 265-271.
- Sato, K. (1991), "On the governing equation for vibrating and stability of a Timoshenko beam: Hamilton's Principle", *J. Sound Vib.*, **145**(2), 338-340.
- Shvartsman, B.S. (2007), "Large deflections of a cantilever beam subjected to a follower force", *J. Sound Vib.*, **304**, 969-973.
- Sugiyama, Y. and Langthjem, M.A. (2007), "Physical mechanism of the destabilizing effect of damping in continuous non-conservative dissipative systems", *Int. J. Non-Linear Mech.*, **42**(1), 132-145.
- Thana, H.K. and Ameen, M. (2007), "Finite element analysis of dynamic stability of skeletal structures under periodic loading", *J. Zhejiang University Science A*, **8**(2), 245-256.
- Tomski, L., Szmidla, J. and Uzny, S. (2007), "The local and global instability and vibration of systems subjected to non-conservative loading", *Thin Wall. Struct.*, **45**, 945-949.
- Tsiatas, G.C. and Katsikadelis, J.T. (2009), "Post-critical behavior of damped beam columns with variable cross-section subjected to distributed follower forces", *Nonlinear Dynam.*, **56**(4), 429-441.
- Wang, Q. and Quek, S.T. (2002), "Enhancing flutter and buckling capacity of column by piezoelectric layers", *Int. J. Solids Struct.*, **39**, 4167-4180.
- Wang, Q. (2004), "A comprehensive stability analysis of a cracked beam subjected to follower compression", *Int. J. Solids Struct.*, **41**, 4875-4888.
- Wu, J.J. (1975), "On the stability of a free-free beam under axial thrust subjected to directional control", *J. Sound Vib.*, **43**(1), 45-52.
- Young, T.H. and Juan, C.S. (2003), "Dynamic stability and response of fluttered beams subjected to random follower forces", *Int. J. Non-Linear Mech.*, **38**, 889-901.
- Zuo, Q.H. and Schreyer, H.L. (1996), "Flutter and divergence instability of nonconservative beams and plates", *Int. J. Solids Struct.*, **33**(9), 1355-1367.